A Dual-Mode Hybrid System Combining Solar Thermal With Pumped Thermal Energy Storage

Joshua McTigue[1] , and Zhiwen Ma[1]

[1] National Renewable Energy Laboratory, USA

* Correspondence: Joshua McTigue, jmctigue_nrel@outlook.com

Abstract. A hybrid system that delivers renewable electricity generation and electricity storage capabilities is introduced. This dual-mode hybrid system is based on Pumped Thermal Energy Storage (PTES) which uses a heat pump to convert electricity into thermal energy that is transferred to silica particles which are stored in concrete silos. The stored heat is later converted back to electricity in a heat engine. The heat pump and heat engine use a closed Joule-Brayton cycle and fluidized bed heat exchangers. If the PTES system is co-located with an array of concentrating solar mirrors and a particle receiver, then the silica particles may also be heated up by the concentrating solar power (CSP) system. The PTES heat engine may also be used to convert the stored solar heat into electricity, thereby sharing this system between the PTES and CSP systems and reducing costs. However, this requires careful management of the heat engine off-design parameters. A thermodynamic model is used to evaluate the performance of the dual mode PTES-CSP hybrid system. The model accounts for turbomachinery efficiency, and approach temperature and pressure loss in heat exchangers, as well as other sources of inefficiency, such as motor-generator losses, and air fan power. The hybrid system also requires the evaluation of the turbomachinery efficiency and pressure ratio at off-design conditions since the CSP system operates over different temperature ratios than the Carnot Battery. Several design variables and design modifications are investigated, such as pressure ratios and maximum temperatures.

Keywords: Concentrating Solar Thermal Power, Pumped Thermal Energy Storage, Carnot Battery, Particle Thermal Energy Storage, Turbomachinery

1. Introduction

Long duration energy storage (LDES) systems are being developed to provide flexibility and reliability to the electrical grid. By managing electricity supply and demand over a range of temporal durations (from hours to weeks), LDES can support the increased proportions of variable renewable energy generation that are necessary to reduce carbon dioxide emissions [1]. While a variety of LDES technologies are being developed (such as pumped hydro-electric storage, compressed air energy storage, and gravity storage), of particular interest here is a system known as Pumped Thermal Energy Storage (PTES) or a Carnot Battery [2]. PTES uses thermal energy storage (TES) and thermal power cycles and therefore has considerable overlap with technologies developed for the concentrating solar power (CSP) industry. The development of PTES systems can be potentially accelerated by leveraging advances made by the CSP industry. Furthermore, CSP and PTES may be readily hybridized by sharing similar components and it is expected that hybridization could provide economic and operational advantages.

Some PTES concepts may benefit from developments in the CSP industry, such as those that use molten salt TES [3] and particle TES [4]. Molten-salt PTES (MS-PTES) systems use liquid storage tanks and conventional heat exchangers. However, these systems are constrained by the limited operating temperature range of suitable storage liquids and also require very large heat exchange surfaces to achieve a good round-trip efficiency [5]. Silica particles are stable over a wide range of temperatures [6], and consequently, Particle-PTES (P-PTES) systems may be operated at higher temperatures and therefore with a higher round-trip efficiency [4]. Silica particles are also low cost and abundant [7-9], and can exchange heat directly in Fluidized Bed Heat Exchangers (FBHX), thereby avoiding the cost of metal heat transfer surfaces [10]. However, advancements are required to develop particle conveyance systems.

In this article, a hybrid PTES-CSP system is introduced in which the power cycle, heat exchangers, heat rejection system, TES, and grid connection are shared between the two systems. It is expected that combining these systems will reduce costs compared to two-standalone systems and enable the system to provide a range of energy management services and therefore 'stack' revenue streams [11]: for example, this system can provide both long-duration electricity storage services and renewable power generation. These advantages have to be weighed against the additional complexity of designing, constructing, and operating such a hybrid plant. Furthermore, unlike stand-alone PTES, hybrid PTES-CSP has geographical constraints.

Previous work that has examined the integration of solar heat with Joule-Brayton PTES have focused on systems that use molten salt TES [12]. For example, Ref. [13] introduced the concept of using a heat pump to add thermal energy to the TES at an existing CSP installation. In this case, retrofitting a CSP system with a heat pump increases the value that the plant can provide. It also enables PTES concepts to be developed and deployed at reduced costs as the TES and power cycle have already been installed. Existing CSP systems have steam Rankine cycles whereas Ref. [13] proposed the use of a Joule-Brayton heat pump which leads to some complications in system design. Alternatively, a heat pump could be used to upgrade the temperature produced by a CSP system. For example, Ref. [14] proposed using a heat pump powered by solar photovoltaics to increase the temperature from a parabolic trough collector, which is then stored in molten salts and converted to electricity using a steam cycle.

In this article, a thermodynamic model is used to evaluate the performance of the hybrid PTES-CSP system. A key aspect of the model is the evaluation of the turbomachinery efficiency and pressure ratio at off-design conditions since the CSP system operates over different pressure ratios to the PTES. Off-design turbomachinery maps are used and a control method known as inventory control is used to find operating points at off-design conditions. Several design variables and design modifications are investigated, such as maximum temperatures, pressure ratios and number of compression stages. While some factors uniformly improve performance (such as increasing maximum temperatures), some variables result in trade-offs between different objectives requiring a compromise to be made for system performance. The choice of some design decisions result in a trade-off between the PTES and CSP performance so that a compromise must be made between the performance of the two systems.

2. System Description

The hybrid system described here has two operating modes: (1) Electricity storage mode using PTES (2) Electricity generation mode using CSP. PTES-mode has a charge phase and a discharge phase. First, thermal energy storage is charged with a heat pump that is powered by grid electricity. Importantly, the heat pump extracts energy from one thermal reservoir thereby creating a cold storage and upgrades this heat to higher temperatures that are stored in another thermal reservoir, to create a hot storage. Later, the discharging phase uses a heat engine that operates between the two thermal reservoirs to generate electricity. Here, the heat

pump and heat engine use a closed Joule-Brayton cycle with nitrogen working fluid [15]. Energy is stored in silica particles which are stored in large concrete silos and heat is transferred between the particles and thermal cycles using Fluidized Bed Heat Exchangers. This particle-PTES concept was introduced and modelled at the SolarPACES 2022 conference [4]. A system schematic and corresponding temperature-entropy diagram are shown in Figure 1a and Figure 2a.

The charging heat pump operation is as follows: a gas is compressed from temperature T_1 to T_2 in the compressor and then enters the FBHX where it transfers heat to the particles and is cooled T_3. The cool, high-pressure gas is expanded in a turbine to sub-ambient temperature T_4 before entering a second FBHX where it cools another set of particles which return the gas to temperature T_1. As can be deduced from Figure 2a, the 'cold' storage particles operate between a sub-ambient temperature (~-25°C) and a hot temperature (~540°C).

In the discharging heat engine, the gas flow direction is reversed compared to the heat pump. While the same heat exchangers are used, an additional set of turbomachinery is required (although reversing turbomachinery designs are being developed). The pressure ratio of the discharging cycle is chosen to ensure that both the hot and cold particles are returned to their original temperatures. As a result, the discharging pressure ratio is larger than the charging pressure ratio. Some heat (the result of irreversibilities) is also rejected during discharge.

The PTES performed is assessed by the round-trip efficiency η_{RT}; simply defined as the fraction of input electricity $W_{\mathrm{in}}^{\mathrm{chg}}$ that is recovered during discharge $W_{\mathrm{out}}^{\mathrm{dis}}$:

$$\eta_{\mathrm{RT}} = \frac{W_{\mathrm{out}}^{\mathrm{dis}}}{W_{\mathrm{in}}^{\mathrm{chg}}} \tag{1}$$
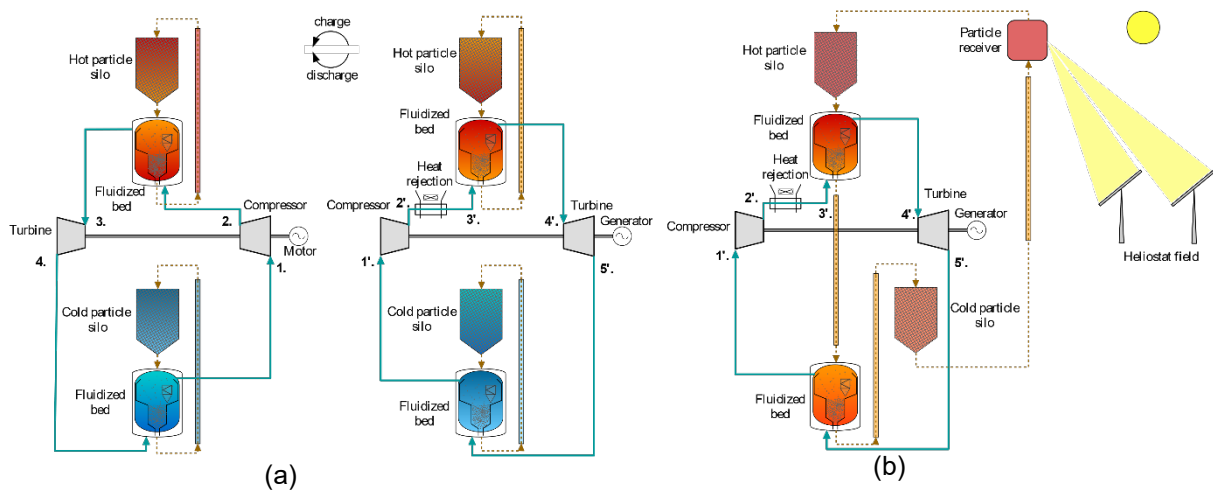

Figure 1. *(a) Schematic illustrating PTES using particle thermal energy storage. (b) Schematic illustrating a solar thermal heat engine using the same components as PTES*
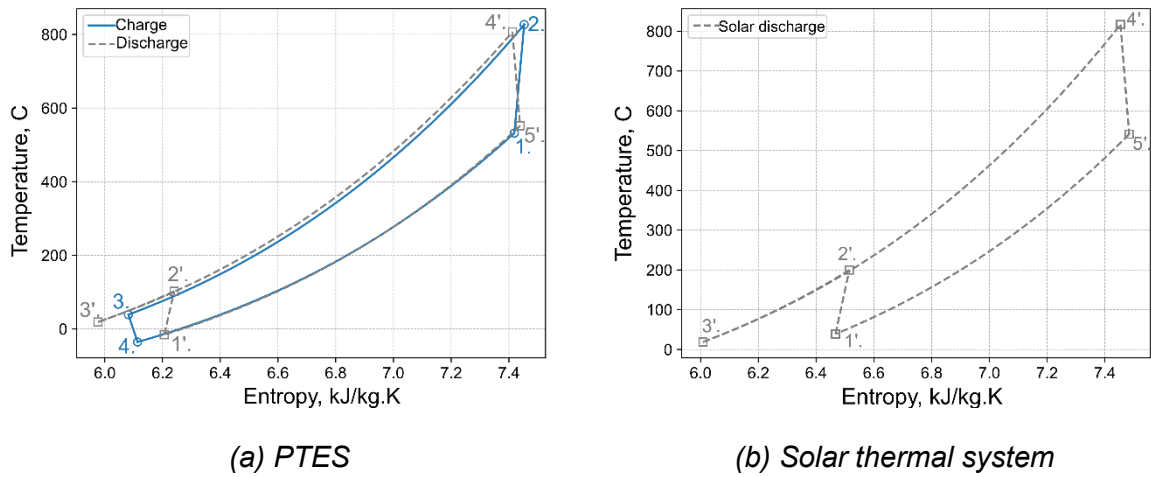
(a) PTES *(b) Solar thermal system*

Figure 2. *Temperature-entropy diagrams of PTES and solar thermal system. Numbering corresponds to Figure 1.*

The CSP-mode has a charge phase in which solar thermal energy is used to heat particles in a particle receiver. The particles are then stored in a concrete silo. The CSP-mode discharge phase uses a heat engine to convert the stored thermal energy to electricity. Notably, the CSP-mode heat engine uses the same set of components (turbomachinery, thermal storage, heat exchangers, and generator) as the PTES-mode heat engine. The power cycle working fluid traverses the turbomachinery and FBHXs in the same order as PTES-mode to reduce additional pipes and values, and the particles are moved in such a way that at the end of CSP mode, the particles are at the right temperature to be used in either PTES-mode or CSP-mode. An important aspect of CSP-mode is that cold storage is not available, so the compressor inlet temperature is close to ambient temperature, and is therefore considerably warmer than the inlet temperature during PTES-mode. However, the 'cold' FBHX is still used in CSP-mode and this requires an extra particle lift to move particles from the hot FBHX to the cold FBHX. This arrangement ensures that the working fluid follows the same sequence of components as in PTES-mode discharge. The particles now provide recuperation from one side of the cycle to the other, which reduces the temperature range over which solar heat is added to the cycle, therefore improving the heat engine efficiency. A system schematic and corresponding temperature-entropy diagram are shown in Figure 1b and Figure 2b.

The performance of the CSP-mode is assessed by the heat engine efficiency η_{HE}, where

$$\eta_{HE} = \frac{W_{\text{out}}^{\text{dis}}}{Q_{\text{solar}}} \tag{2}$$

3. Modelling Methods

A thermodynamic model is used to assess the performance of the PTES-CSP hybrid system. The model uses simple assumptions for each of the components:

- Compressors and expanders are assumed to be on the same shaft and are modelled with a polytropic efficiency η_p
- The working fluid is nitrogen and fluid properties are calculated with CoolProp [16] since the heat capacity does vary appreciably over the range of temperatures considered
- The FBHXs are modelled using an average approach temperature ΔT and a fractional pressure loss
- Motors and generators are modelled with an efficiency term

- The electrical work input to cooling fans is calculated by considering the air pressure loss and the fan efficiency

Table 1. Nominal design inputs and performance

Parameter		Value
Charge compressor polytropic efficiency	%	90.7
Charge expander polytropic efficiency	%	87.7
Discharge compressor polytropic efficiency	%	93.3
Discharge expander polytropic efficiency	%	92.0
Hot HX approach temperature	K	10
Cold HX approach temperature	K	10
Heat rejection approach temperature	K	4
Hot HX pressure loss	%	2.5
Cold HX pressure loss	%	2.5
Heat rejection pressure loss	%	0.5
Motor efficiency	%	97.22
Generator efficiency	%	97.22
Fan efficiency	%	70.0
Charge compressor inlet pressure	bar	5
Charge compressor pressure ratio		3
Charge compressor inlet temperature	K	805
Charge compressor outlet temperature	K	1100
Solar heat addition temperature	K	1100
Ambient temperature	K	288
PTES round-trip efficiency	%	61.4
CSP heat engine efficiency	%	42.7

Assumptions are provided in Table 1 which is based on the PTES system described in Ref. [4] in which the model is described in more detail. In this work, the model is updated to include off-design performance maps for the compressors and turbines. Changes to the inlet or outlet conditions (mass flow rates, temperatures, or pressures) affect the pressure ratio and efficiency of the turbomachines. Characteristic curves were obtained for air-based tur-bomachinery from Refs. [17-19] and are functions that relate the pressure ratio and efficiency to the mass flow rate, rotational speed, inlet pressure and inlet temperature.
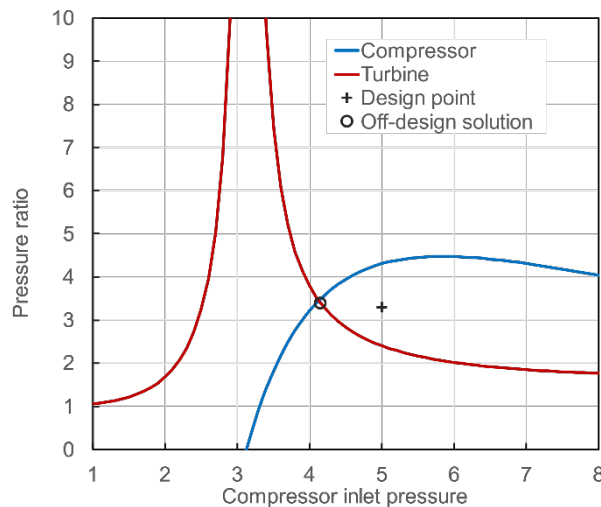

Figure 3. *Off-design characteristics of the discharging compressor and turbine. The compressor inlet temperature is increased and the inlet pressure is then varied to find a solution in which the compressor and turbine off-design pressure ratios are equal.*

The cycles of interest are closed gas cycles and it is therefore important that the compressor and turbine pressure ratios 'match' – i.e. the pressure ratios should be approximately equal (depending on other sources of pressure loss in the system). The system is further constrained as the compressor and turbine are on the same shaft and therefore rotate at the same speed. One method of operating the cycle under off-design conditions is known as inventory control which aims to maintain a constant volumetric flow rate through the turbomachines. This is equivalent to keeping the mass flow coefficient, $\dot{m}_c = \dot{m}\sqrt{T}\,/\,p$, constant. By varying the mass flow rate and inlet pressure, it is possible to achieve only small changes in the mass flow coefficient, and therefore to keep the turbomachine efficiency and pressure ratio relatively close to the design value, as described in Ref. [20]. Previous work has shown that the power output and round-trip efficiency does not change significantly when using inventory control over a wide range of part-load conditions [20,21]. Other methods of off-design control include turbomachinery speed control [22], recycling working fluid and storage fluids [23], and varying storage fluid mass flow rates. These methods are useful for managing off-design conditions and for system start up.

Here, inventory control is used to enable the system to operate in either CSP-mode or PTES-mode. The design conditions are set by the PTES mode, and the discharge compressor inlet temperature and pressure are -15°C and 5 bar, respectively, with a pressure ratio of 3.3. However, in CSP-mode, the compressor inlet temperature is 39°C because cold storage is not available. The change in inlet temperature affects the compressor pressure ratio and efficiency. This consequently impacts the turbine inlet conditions and thus, the turbine pressure ratio which may no longer match the compressor pressure ratio. Inventory control is used to change the compressor inlet temperature and match the turbomachinery pressure ratios. Figure 3 illustrates how the off-design pressure ratios depend on the compressor inlet pressure and demonstrate that it is possible to find a solution in which the off-design pressure ratios of the compressor and turbine match. In this case, the compressor inlet pressure reduces from 5 to 4.2, and the pressure ratio changes slightly from 3.3 to 3.4. Operating CSP-mode in this way reduces the turbomachinery efficiency slightly which impacts the overall performance of the CSP heat engine. Further work is required to understand the long term practical impacts of operating turbomachinery in this way.

4. Results

Key parameters for hybrid PTES-CSP performance are the maximum temperature of the system and the pressure ratio. These parameters are varied in Figure 4 while keeping other variables fixed at the values shown in Table 1. These results demonstrate that the efficiency of each mode is optimized at different pressure ratios: optimal CSP mode efficiencies occur at lower pressure ratios than PTES round-trip efficiency. Increasing the maximum cycle temperature increases the efficiency and power output of both modes. It is notable that the efficiency curves for CSP mode are relatively steep: choosing a pressure ratio slightly different to the optimal value substantially reduces the efficiency. On the other hand, the PTES curves are relatively flat which indicates it may be preferable to reduce the PTES-mode performance a small amount in order to achieve reasonable CSP-mode performance.

As described in the Modelling Methods section, CSP-mode requires the turbomachinery to be operated at off-design conditions which reduces the turbomachinery efficiency. Figure 5 shows how the turbomachinery efficiency in CSP-mode varies with design PTES-mode pressure ratio. Turbomachinery efficiency is always reduced in CSP-mode but this effect is less significant for low design pressure ratios.

The CSP-mode efficiency is relatively low given the turbine inlet temperature, but performance can be improved by modifying the cycle design. Firstly, multiple intercooled compressions during discharge reduce the total compression work and therefore increase the efficiency and power output. Any changes to the system architecture for the CSP heat engine

6

must be reflected in the PTES design (since the turbomachinery is shared between the two modes). As a result, the PTES system has multiple intercooled compressions during discharge, and an equal number of inter-heated expansions in the charging heat pump. Figure 6a demonstrates that multiple discharge compressions improves the CSP-mode efficiency. However, they have a detrimental impact on PTES mode: multiple charge expansions in the heat pump increase the temperature of the cold storage which has the net effect of reducing the round-trip efficiency (compare the *T-s* diagram of Figure 7 with Figure 2a). Therefore, the decision to use multiple compressions leads to a trade-off between the performance of the two modes, although it appears that improvements to CSP-mode are larger than the reduction in PTES-mode performance. A further consideration is that multiple discharging compressions increases the system complexity and cost, as additional heat exchangers and heat rejection equipment is required.
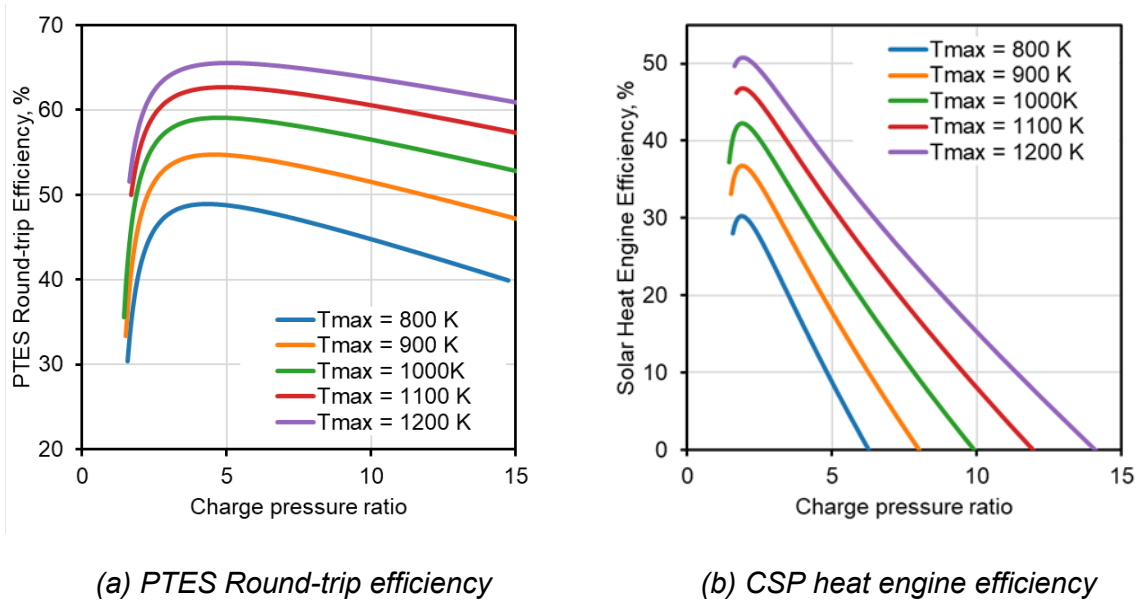

(a) PTES Round-trip efficiency   *(b) CSP heat engine efficiency*

Figure 4. *Hybrid PTES-CSP efficiency as a function of pressure ratio and maximum temperature*
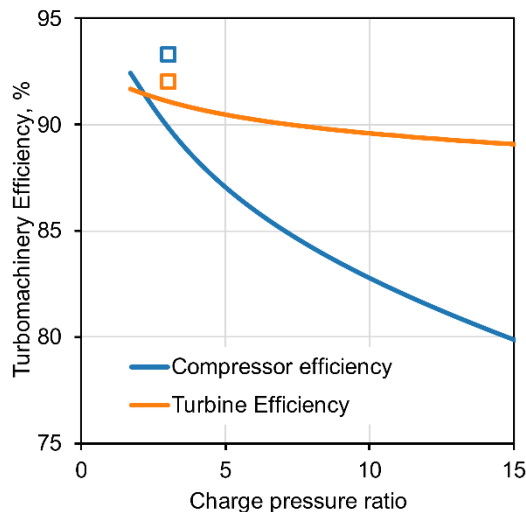

Figure 5. *Off-design turbomachinery efficiency in the CSP system as a function of design pressure ratio. Design values are shown as square markers.*

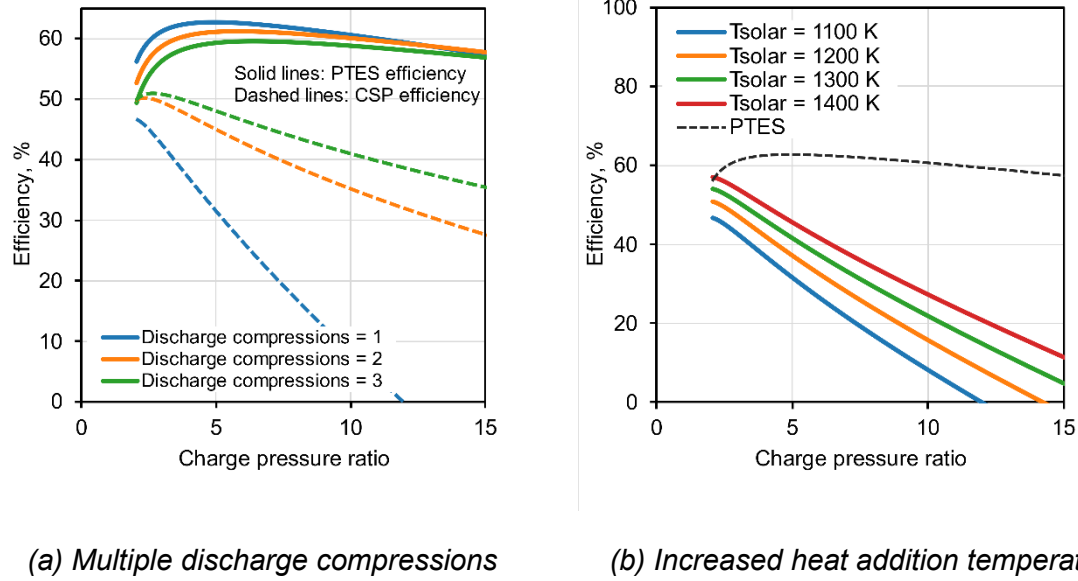(a) Multiple discharge compressions (b) Increased heat addition temperature

Figure 6. *Performance of hybrid CSP-PTES systems with design modifications. Pressure ratio is varied along the curves while the PTES maximum temperature is fixed at 1100K*
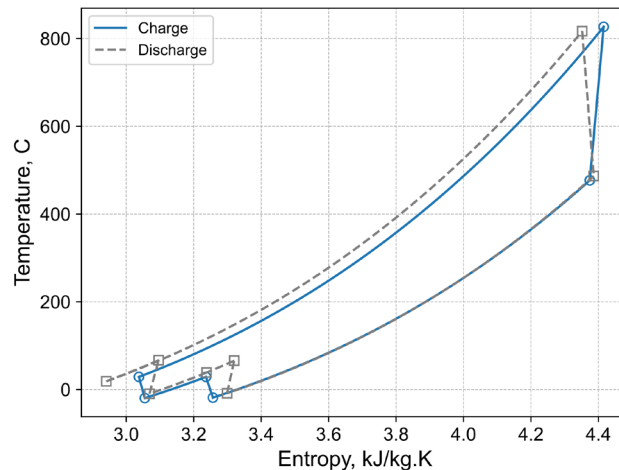

Figure 7. *Temperature-entropy diagram of a Carnot Battery with multiple discharge compressions (and corresponding charge expansions).*

Another modification that improves the CSP-mode efficiency is to use the solar heat to charge the hot particles to higher temperatures than the heat pump. Conceivably, the same particles and storage silos can still be used in both modes due to the particle stability over wide temperature ranges. Therefore, the CSP-mode performance is improved due to an increased turbine inlet temperature. One challenge is that the discharging turbine will have different inlet temperatures during PTES mode and CSP mode. However, the inventory control method (i.e. moderating the cycle pressure) can again be used to ensure the compressor and turbine pressure ratios are matched – at the expense of reducing turbomachinery efficiency. Results are shown in Figure 6b for a system with a maximum heat pump temperature of 1100K. In CSP-mode, the solar heat is added at temperatures greater than or equal to 1100K. Clearly, increasing the maximum solar temperature improves both the heat engine efficiency and power output despite operating at off-design conditions. Furthermore, this modification does not affect PTES performance so design trade-offs are not required.

The performance of three specific design cases is given in Table 2. The first column shows results for a system where the PTES performance is prioritized, which results in a low CSP-mode efficiency. The second column illustrates the performance of a system where CSP-mode is prioritized at the expense of PTES-mode. The pressure ratio is reduced and multiple discharge compressions are introduced. This significantly increases the CSP-mode efficiency, while slightly reducing PTES-mode performance to 56.7% which is a reasonable value. The third column of Table 2 shows results for a compromise for the hybrid CSP-PTES design where design variables are carefully chosen to balance the performance of the two systems. This system does not have multiple compression stages to minimize complexity. This system achieves good performance for both systems with $\eta_{RT} = 60.9\%$ and $\eta_{HE} = 54.9\%$. The performance is further improved by making aggressive assumptions for approach temperatures, pressure losses, and solar heat addition temperatures, see the fourth column.

***Table 2.** Performance of three hybrid designs*

		Prioritize PTES-mode	Prioritize CSP-mode	Compro-mise	Optimistic design
Approach temp.	K	10	10	10	5
Pressure loss	%	2.5	2.5	2.5	1.0
Charge pressure ratio	-	4.8	2.7	2.8	2.8
Max. PTES temp.	K	1100	1100	1100	1100
Max. solar temp.	K	1100	1400	1400	1400
Number of compressions		1	3	1	1
PTES η_{rt}	%	63.0	55.3	60.9	70.0
CSP η_{HE}	%	32.9	60.6	54.9	57.5

5. Conclusions

A dual-mode hybrid system is introduced in this article. The system combines Pumped Thermal Energy Storage (PTES) with Concentrating Solar Power (CSP) and shares several key components between them, including thermal energy storage, heat exchangers, turbomachines, and generator. By sharing components in this way, the hybrid system can provide both electricity storage services and renewable power generation at reduced cost compared to two stand-alone systems.

A thermodynamic model is used to evaluate the performance of the dual-mode hybrid system. Sharing the heat engine between the two modes requires it to operate at conditions that are significantly far from the design point. This is challenging because the closed Joule-Brayton cycle requires the pressure ratios and rotational speeds of the compressor and expander to be matched. A method – based on inventory control – is described, in which the compressor inlet pressure is carefully chosen to ensure that the turbomachinery pressure ratios match. This comes with a small efficiency penalty but facilitates the use of the heat engine in two different systems.

Key design variables are investigated including the charge pressure ratio and maximum PTES temperature. Increasing the maximum temperature improves the performance of both PTES-mode and CSP-mode. However, each mode is optimized at a different value of pressure ratio. It is noted that CSP-mode is more sensitive to the pressure ratio, so a compromise can be reached in which CSP-mode efficiency is improved without significantly reducing PTES-mode efficiency.

CSP-mode efficiency may also be improved by using multiple intercooled compressions in the heat engine. However, this reduces PTES-mode efficiency as well as increasing the complexity and cost of the system due to the need for multiple compressors, heat exchangers, and expanders. The particle solar receiver can conceivably heat the particles to higher

temperatures than the PTES heat pump. Therefore, CSP-mode efficiency is increased if the temperature of solar heat addition is maximized. This modification does not affect PTES-mode efficiency although it requires that particle silos and transport technology is designed for higher temperatures. Results indicate that by carefully choosing design variables, the hybrid system can achieve good efficiencies in both modes – e.g. PTES-mode round-trip trip efficiency of 60.9% and CSP-mode heat engine efficiency of 54.9%.

Data availability statement

Data is available upon request to the authors.

Author contributions

Joshua McTigue: Conceptualization, Methodology, Analysis, Writing – Original Draft, Visualization **Zhiwen Ma**: Conceptualization, Supervision, Funding Acquisition, Writing – Outline and Draft Revision.

Competing interests

The authors declare no competing interests.

Acknowledgement and Funding

Funding

References

[1]   International Energy Agency, Net Zero by 2050: A Roadmap for the Global Energy Sector, 2021. iea.li/nzeroadmap.
[2]   A. Olympios, J. McTigue, P. Farres-Antunez, A. Romagnoli, W. Steinmann, A. Thess, L. Wang, H. Chen, Y. Li, Y. Ding, C. Markides, Progress and prospects of thermo-mechanical energy storage – a critical review, IOP Prog. Energy. 3 (2021). https://doi.org/10.1088/2516-1083/abdbba.
[3]   R.B. Laughlin, Pumped thermal grid storage with heat exchange, J. Renew. Sustain. Energy. 9 (2017). https://doi.org/10.1063/1.4994054.
[4]   J.D. McTigue, Z. Ma, Pumped Thermal Energy Storage with Particle Silos and Fluidized Bed Heat Exchangers, in: SolarPACES 2022, Albuquerque, New Mexico, 2022.
[5]   J.D. McTigue, P. Farres-Antunez, K. Sundarnath J, C.N. Markides, A.J. White, Techno-economic analysis of recuperated Joule-Brayton pumped thermal energy storage, Energy Convers. Manag. 252 (2022). https://doi.org/10.1016/j.enconman.2021.115016.

[6]   P. Davenport, Z. Ma, J. Schirck, W. Nation, A. Morris, X. Wang, M. Lambert, Characterization of solid particle candidates for application in thermal energy storage and concentrating solar power systems, Sol. Energy. 262 (2023) 111908. https://doi.org/10.1016/j.solener.2023.111908.

[7]   Z. Ma, R. Zhang, F. Sawaged, Design of a Particle-Based Thermal Energy Storage for a Concentrating Solar Power System, in: Proc. ASME 2017 11th Int. Conf. Energy Sustain., Charlotte, North Carolina, 2018: pp. 1–8.

[8]   Z. Ma, X. Wang, P. Davenport, J. Gifford, J. Martinek, J. Schirck, A. Morris, M. Lambert, R. Zhang, System and Component Development for Long-Duration Energy Storage, Appl. Therm. Eng. (2022) 119078. https://doi.org/10.1016/j.applthermaleng.2022.119078.

[9]   Z. Ma, J. Martinek, C. Turchi, J. McTigue, J. Sment, C. Ho, Thermal energy storage for energy decarbonization, Annu. Rev. Heat Transf. (2022) 51–115.

[10]   Z. Ma, X. Wang, P. Davenport, J. Gifford, J. Martinek, Economic analysis of an electric thermal energy storage system using solid particles for grid electricity storage, Proc. ASME 2021 15th Int. Conf. Energy Sustain. ES 2021. (2021). https://doi.org/10.1115/ES2021-61729.

[11]   J.D. McTigue, P. Farres-Antunez, C.N. Markides, A.J. White, Integration of heat pumps with solar thermal systems for energy storage, in: Encycl. Energy Storage, Elsevier, 2022. https://doi.org/10.1016/B978-0-12-819723-3.00131-1.

[12]   J.D. McTigue, P. Farres-Antunez, A.J. White, C.N. Markides, J. Martinek, J. Jorgenson, T. Neises, M. Mehos, Integrated Heat Pump Thermal Storage and Power Cycle for CSP : Final Technical Report, NREL Tech. Rep. - NREL/TP-5700-79806. (2022). https://www.nrel.gov/docs/fy22osti/79806.pdf.

[13]   P. Farres-Antunez, J.D. McTigue, A.J. White, A pumped thermal energy storage cycle with capacity for concentrated solar power integration, in: 2019 Offshore Energy Storage Summit, OSES 2019, 2019. https://doi.org/10.1109/OSES.2019.8867222.

[14]   Z. Mahdi, J. Dersch, P. Schmitz, S. Dieckmann, R. Alexander, C. Caminos, C. Teixeira Boura, U. Herrmann, C. Schwager, M. Schmitz, H. Gielen, Y. Gedle, R. Büscher, Technical Assessment of Brayton Cycle Heat Pumps for the Integration in Hybrid PV-CSP Power Plants, SolarPACES. (2020).

[15]   A. V Olympios, J.D. McTigue, P. Sapin, C.N. Markides, E. Processes, Pumped-Thermal Electricity Storage Based on Brayton Cycles, Elsevier Inc., 2021. https://doi.org/10.1016/B978-0-12-819723-3.00086-X.

[16]   I.H. Bell, J. Wronski, S. Quoilin, V. Lemort, Pure and Pseudo-pure Fluid Thermophysical Property Evaluation and the Open-Source Thermophysical Property Library CoolProp, Ind. Eng. Chem. Res. 53 (2014) 2498–2508. https://doi.org/10.1021/ie4033999.

[17]   A. Sciacovelli, Y. Li, H. Chen, Y. Wu, J. Wang, S. Garvey, Y. Ding, Dynamic simulation of Adiabatic Compressed Air Energy Storage (A-CAES) plant with integrated thermal storage – Link between components performance and plant performance, Appl. Energy. 185 (2017) 16–28. https://doi.org/10.1016/j.apenergy.2016.10.058.

[18]   L.S. Dixon, C.A. Hall, Fluid Mechanics and Thermodynamics of Turbomachinery, Elsevier Science, 2010.

[19]   N. Zhang, R. Cai, Analytical solutions and typical characteristics of part-load performances of single shaft gas turbine and its cogeneration, Energy Convers. Manag. 43 (2002) 1323–1337. https://doi.org/10.1016/S0196-8904(02)00018-3.

[20]   J.D. McTigue, P. Farres-Antunez, C.N. Markides, A.J. White, Pumped thermal energy storage with liquid storage, in: Encycl. Energy Storage, 2021. https://doi.org/doi:10.1016/B978-0-12-819723-3.00054-8.

[21]   G.F. Frate, L. Paternostro, L. Ferrari, U. Desideri, Off-Design of a Pumped Thermal Energy Storage Based on Closed Brayton Cycles, in: Proc. ASME Turbo Expo 2-21, 2021: pp. 1–14.

[22]   C. Lu, X. Shi, Q. He, Y. Liu, X. An, S. Cui, D. Du, Dynamic modeling and numerical investigation of novel pumped thermal electricity storage system during startup process, J. Energy Storage. 55 (2022) 105409. https://doi.org/10.1016/j.est.2022.105409.

[23]   N.R. Smith, J. Just, J. Johnson, F.K. Bulnes, Performance Characterization of a Small-Scale Pumped Thermal Energy Storage System, in: Proc. ASME Turbo Expo, Boston, MA, 2023: pp. 1–12.